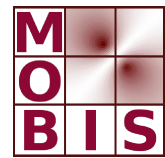




SpezialForschungsBereich F 32



Karl-Franzens Universität Graz
Technische Universität Graz
Medizinische Universität Graz



FETI Methods for the Simulation of Biological Tissues

Ch. Augustin O. Steinbach

SFB-Report No. 2011-011

May 2011

A-8010 GRAZ, HEINRICHSTRASSE 36, AUSTRIA

Supported by the
Austrian Science Fund (FWF)

FWF Der Wissenschaftsfonds.

SFB sponsors:

- **Austrian Science Fund (FWF)**
- **University of Graz**
- **Graz University of Technology**
- **Medical University of Graz**
- **Government of Styria**
- **City of Graz**



FETI Methods for the Simulation of Biological Tissues

Christoph Augustin and Olaf Steinbach

Abstract In this paper we describe the application of finite element tearing and interconnecting methods for the simulation of biological tissues which are characterized by anisotropic and nonlinear materials.

1 Modeling Biological Tissues

In this paper we consider the numerical simulation of biological tissues, that can be described by the stationary equilibrium equations

$$\operatorname{div} \sigma(u, x) + f(x) = 0 \quad \text{for } x \in \Omega \subset \mathbb{R}^3, \quad (1)$$

to find a displacement field u where we have to incorporate boundary conditions to describe the displacements or the boundary stresses on $\Gamma = \partial\Omega$.

In the case of biological tissues the material is assumed to be hyperelastic, i.e. we have to incorporate large deformations and a non-linear stress-strain relation. For the derivation of the constitutive equation we introduce the strain energy function $\Psi(\mathbf{F})$ which represents the elastic stored energy per unit reference volume. From this we obtain the constitutive equation as in [1]

$$\sigma = J^{-1} \mathbf{F} \frac{\partial \Psi(\mathbf{C})}{\partial \mathbf{C}} \mathbf{F}^\top,$$

where $J = \det \mathbf{F}$ is the Jacobian of the deformation gradient $\mathbf{F} = \nabla_x \varphi(x)$, and $\mathbf{C} = \mathbf{F}^\top \mathbf{F}$ is the right Cauchy-Green tensor. In what follows we make use of the Rivlin-Ericksen representation theorem to find a representation of the strain energy function Ψ in terms of the principal invariants of $\mathbf{C} = \mathbf{F}^\top \mathbf{F}$.

Christoph Augustin · Olaf Steinbach
Institute of Computational Mathematics, TU Graz, Steyrergasse 30, 8010 Graz, Austria,
e-mail: caugustin@tugraz.at, o.steinbach@tugraz.at

Arteries are composed of three layers: the intima, the media, and the adventitia. In the case of a healthy young artery, the innermost layer, the intima, is not of mechanical interest. Each of the other layers is modeled with a separate strain-energy function. We assume that the media as well as the adventitia respond with similar mechanical characteristics and therefore we use the same form of the related strain-energy functions Ψ . To capture the specifics of each layer, a different set of material parameters is used. Each layer of the artery is modeled as a fiber-reinforced composite. In particular, the strain-energy function Ψ is decomposed into a volumetric part, an isotropic and an anisotropic part, see [5],

$$\Psi(\mathbf{C}) = \frac{\kappa}{2} (J - 1)^2 + \Psi_{\text{iso}}(\mathbf{C}) + \Psi_{\text{aniso}}(\mathbf{C}, \mathbf{A}_1, \mathbf{A}_2), \quad (2)$$

where the two given symmetric structure tensors \mathbf{A}_1 and \mathbf{A}_2 are constructed by the two main directions of the collagen fibers in the arterial wall β_1, β_2 . To model the non-collagenous, isotropic ground substance, mainly consisting of elastin, we use the classical Neo-Hookean model

$$\Psi_{\text{iso}}(\mathbf{C}) = \Psi_{\text{iso}}(I_1) = \frac{c}{2} (J^{-2/3} I_1 - 3), \quad (3)$$

where $c > 0$ is a stress-like material parameter, and $I_1 = \text{tr}(\mathbf{C})$ is the first principal invariant of the right Cauchy-Green tensor \mathbf{C} . In (2), Ψ_{aniso} is associated with the anisotropic deformations arising from the collagen fibers. Following [5] we describe the anisotropic response by using

$$\Psi_{\text{aniso}}(\mathbf{C}, \mathbf{A}_1, \mathbf{A}_2) = \frac{k_1}{2k_2} \sum_{i=4,6} \left\{ \exp[k_2 (J^{-2/3} I_i - 1)^2] - 1 \right\}, \quad (4)$$

where $I_4 = \mathbf{C} : \mathbf{A}_1$, $I_6 = \mathbf{C} : \mathbf{A}_2$, and the material parameters k_1 and k_2 are assumed to be positive. Note that all appearing constants can be fitted to an experimentally observed response of the arterial layers.

It is worth to mention, that in this model the anisotropic response Ψ_{aniso} only contributes in the cases $I_i > 1$, $i = 4, 6$. This corresponds to a stretch in a fiber direction, and this is explained by the wavy structure of the collagen fibers. In particular, the collagen fibers are not able to support compressive stress. Moreover, the collagen fibers are not active at low pressure, and the material behaves isotropically in this case. In contrast, at high pressure the collagen fibers straighten and then they govern the resistance to stretch of the material. This behavior of biological tissues was observed in experiments and this is fully covered by the artery model as described above. The stiffening effect at higher pressure also motivates the use of the exponential function in the anisotropic response of the strain energy Ψ .

Note that similar models can also be used for the description of other biological materials, e.g., of the myocardium in the cardiac muscle [6].

2 Finite Element Approximation

In this section we consider the variational formulation of the equilibrium equations (1) with Dirichlet boundary conditions $u = g_D$ on Γ_D , Neumann boundary conditions $t := \sigma(u)n = g_N$ on Γ_N , $\Gamma = \overline{\Gamma_D} \cup \overline{\Gamma_N}$, $\Gamma_D \cap \Gamma_N = \emptyset$, and n is the exterior normal vector of $\Gamma = \partial\Omega$. In particular we have to find $u \in [H^1(\Omega)]^3$, $u = g_D$ on Γ_D , such that

$$a(u, v) := \int_{\Omega} \sigma(u) : \mathbf{e}(v) \, dx = \int_{\Omega} f \cdot v \, dx + \int_{\Gamma_N} g_N \cdot v \, ds_x =: F(v) \quad (5)$$

is satisfied for all $v \in [H^1(\Omega)]^3$, $v = 0$ on Γ_D .

By introducing an admissible decomposition of the computational domain Ω into tetrahedra and by using piecewise linear basis functions φ_ℓ , the Galerkin finite element discretization of the variational formulation (5) results in a nonlinear system of algebraic equations, to find u_h satisfying an approximate Dirichlet boundary condition $u_h = Q_h g_D$ on Γ_D , and

$$K_\ell(u_h) = \int_{\Omega} \sigma(u_h) : \mathbf{e}(\varphi_\ell) \, dx = \int_{\Omega} f \cdot \varphi_\ell \, dx + \int_{\Gamma_N} t \cdot \varphi_\ell \, ds_x = F_\ell. \quad (6)$$

For the solution of the nonlinear system (6), i.e. of $G(u_h) := K(u_h) - F = 0$, we apply Newton's method to obtain the recursion

$$u_h^{k+1} = u_h^k + \Delta u_h^k, \quad G'_h(u_h^k) \Delta u_h^k = -G(u_h^k),$$

or, by using the definition of $G(\cdot)$,

$$u_h^{k+1} = u_h^k + \Delta u_h^k, \quad K'_h(u_h^k) \Delta u_h^k = -K(u_h^k). \quad (7)$$

For the computation of the linearized stiffness matrix $K'_h(u_h^k)$ we need to evaluate the derivative of the nonlinear material model as described in the previous section. For a detailed presentation how to compute $K'_h(u_h^k)$ in this particular case we refer to [4].

3 Finite Element Tearing and Interconnecting

For the parallel solution of (7) we will use the finite element tearing and interconnecting approach [3], see also [7, 10] and references given therein.

For a bounded domain $\Omega \subset \mathbb{R}^3$ we introduce a non-overlapping domain decomposition

$$\overline{\Omega} = \bigcup_{i=1}^p \overline{\Omega}_i \quad \text{with } \Omega_i \cap \Omega_j = \emptyset \quad \text{for } i \neq j, \quad \Gamma_i = \partial\Omega_i. \quad (8)$$

The local interfaces are given by $\Gamma_{ij} := \Gamma_i \cap \Gamma_j$ for all $i < j$. The skeleton of the domain decomposition (8) is denoted as

$$\Gamma_C := \bigcup_{i=1}^p \Gamma_i = \Gamma \cup \bigcup_{i < j} \overline{\Gamma}_{ij}.$$

Instead of the global problem (1) we now consider local subproblems to find the local restrictions $u_i = u|_{\Omega_i}$ satisfying partial differential equations

$$\operatorname{div}(\sigma(u_i)) + f(x) = 0 \quad \text{for } x \in \Omega_i,$$

the Dirichlet and Neumann boundary conditions

$$u_i = g_D \quad \text{on } \Gamma_i \cap \Gamma_D, \quad \sigma(u_i)n_i = g_N \quad \text{on } \Gamma_i \cap \Gamma_N,$$

and the transmission conditions

$$u_i = u_j, \quad t_i + t_j = 0 \quad \text{on } \Gamma_{ij},$$

where $t_i = \sigma(u_i)n_i$ is the local boundary stress, and n_i is the exterior normal vector of the local subdomain boundary $\Gamma_i = \partial\Omega_i$. Note that the local stress tensors $\sigma(u_i)$ are defined locally by using the stress-strain function Ψ as introduced in Sect. 1, and by using localized parameters κ, k_1, k_2, c and fiber directions β_1, β_2 . Hence, by reordering the degrees of freedom, the linearized system (7) can be written as

$$\begin{pmatrix} \mathbf{K}'_{11}(u_{1,h}^k) & & & & \mathbf{K}'_{1C}(u_{1,h}^k)\mathbf{A}_1 & & & & \\ & \cdot & & & & \cdot & & & \\ & & \mathbf{K}'_{pp}(u_{p,h}^k) & & & \mathbf{K}'_{pC}(u_{p,h}^k)\mathbf{A}_p & & & \\ & & & & & & & & \\ \mathbf{A}_1^\top \mathbf{K}'_{C1}(u_{1,h}^k) \cdot \mathbf{A}_p^\top \mathbf{K}'_{Cp}(u_{p,h}^k) & & & \sum_{i=1}^p \mathbf{A}_i^\top \mathbf{K}'_{CC}(u_{i,h}^k)\mathbf{A}_i & & & & & \end{pmatrix} \begin{pmatrix} \Delta \mathbf{u}_{1,I}^k \\ \cdot \\ \Delta \mathbf{u}_{p,I}^k \\ \Delta \mathbf{u}_C^k \end{pmatrix} = - \begin{pmatrix} \mathbf{K}_1(u_{1,h}^k) \\ \cdot \\ \mathbf{K}_p(u_{p,h}^k) \\ \sum_{i=1}^p \mathbf{A}_i^\top \mathbf{K}_C(u_{i,h}^k) \end{pmatrix},$$

where the increments $\Delta \mathbf{u}_{i,I}^k$ correspond to the local degrees of freedom within the subdomain Ω_i , and $\Delta \mathbf{u}_C^k$ is related to all global degrees of freedom on the coupling boundary Γ_C .

By introducing the tearing

$$\mathbf{w}_i = \begin{pmatrix} \Delta \mathbf{u}_{i,I}^k \\ \mathbf{A}_i \Delta \mathbf{u}_C^k \end{pmatrix}, \quad \mathbf{K}'_i = \begin{pmatrix} \mathbf{K}'_{ii}(u_{i,h}^k) & \mathbf{K}'_{iC}(u_{i,h}^k) \\ \mathbf{K}'_{Ci}(u_{i,h}^k) & \mathbf{K}'_{CC}(u_{i,h}^k) \end{pmatrix}, \quad \mathbf{f}_i = - \begin{pmatrix} \mathbf{K}_i(u_{i,h}^k) \\ \mathbf{K}_C(u_{i,h}^k) \end{pmatrix},$$

by applying the interconnecting

$$\sum_{i=1}^p \mathbf{B}_i \mathbf{w}_i = \mathbf{0},$$

and by using discrete Lagrange multipliers, we finally have to solve the system

$$\begin{pmatrix} \mathbf{K}'_1 & & & \mathbf{B}_1^\top \\ & \ddots & & \vdots \\ & & \mathbf{K}'_p & \mathbf{B}_p^\top \\ \mathbf{B}_1 & \dots & \mathbf{B}_p & \boldsymbol{\lambda} \end{pmatrix} \begin{pmatrix} \mathbf{w}_1 \\ \vdots \\ \mathbf{w}_p \\ \boldsymbol{\lambda} \end{pmatrix} = \begin{pmatrix} \mathbf{f}_1 \\ \vdots \\ \mathbf{f}_p \\ \mathbf{0} \end{pmatrix}. \quad (9)$$

For the solution of the linear system (9) we follow the standard approach of tearing and interconnecting methods. In the case of a floating subdomain Ω_i , i.e. $\Gamma_i \cap \Gamma_D = \emptyset$, the local matrices \mathbf{K}'_i are not invertible. Hence we introduce the Moore-Penrose pseudo inverse \mathbf{K}_i^\dagger to represent the local solutions as

$$\mathbf{w}_i = \mathbf{K}_i^\dagger (\mathbf{f}_i - \mathbf{B}_i^\top \boldsymbol{\lambda}) + \sum_{k=1}^6 \gamma_{k,i} \mathbf{v}_{k,i}, \quad (10)$$

where $\mathbf{v}_{k,i} \in \ker \mathbf{K}'_i$ correspond to the rigid body motions of elasticity. Note that in this case we also require the solvability conditions

$$(\mathbf{f}_i - \mathbf{B}_i^\top \boldsymbol{\lambda}, \mathbf{v}_{k,i}) = 0 \quad \text{for } i = 1, \dots, 6.$$

In the case of a non-floating subdomain, i.e. $\ker \mathbf{K}_i = \emptyset$, we may set $\mathbf{K}_i^\dagger = \mathbf{K}_i^{-1}$. As in [9] we may also consider an all-floating approach where also Dirichlet boundary conditions are incorporated by using discrete Lagrange multipliers.

In general, we consider the Schur complement system of (9) to obtain

$$\sum_{i=1}^p \mathbf{B}_i \mathbf{K}_i^\dagger \mathbf{B}_i^\top \boldsymbol{\lambda} - \sum_{i=1}^p \sum_{k=1}^6 \gamma_{k,i} \mathbf{B}_i \mathbf{v}_{k,i} = \sum_{i=1}^p \mathbf{B}_i \mathbf{K}_i^\dagger \mathbf{f}_i, \quad (\mathbf{f}_i - \mathbf{B}_i^\top \boldsymbol{\lambda}, \mathbf{v}_{k,i}) = 0,$$

which can be written as

$$\begin{pmatrix} \mathbf{F} & -\mathbf{G} \\ \mathbf{G}^\top & \end{pmatrix} \begin{pmatrix} \boldsymbol{\lambda} \\ \boldsymbol{\gamma} \end{pmatrix} = \begin{pmatrix} \mathbf{d} \\ \mathbf{e} \end{pmatrix} \quad (11)$$

with

$$\mathbf{F} = \sum_{i=1}^p \mathbf{B}_i \mathbf{K}_i^\dagger \mathbf{B}_i^\top, \quad \mathbf{G} = \sum_{i=1}^p \sum_{k=1}^6 \mathbf{B}_i \mathbf{v}_{k,i}, \quad \mathbf{d} = \sum_{i=1}^p \mathbf{B}_i \mathbf{K}_i^\dagger \mathbf{f}_i, \quad \mathbf{e}_{k,i} = (\mathbf{f}_i, \mathbf{v}_{k,i}).$$

For the solution of the linear system (11) we introduce the projection

$$\mathbf{P}^\top := \mathbf{I} - \mathbf{G}^\top (\mathbf{G}\mathbf{G}^\top)^{-1} \mathbf{G}^\top$$

and it remains to consider the projected system

$$\mathbf{P}^\top \mathbf{F}\boldsymbol{\lambda} = \mathbf{P}^\top \mathbf{d} \quad (12)$$

which can be solved by using a parallel conjugate gradient method with suitable preconditioning. Note that the initial approximate solution $\boldsymbol{\lambda}^0$ satisfies the compatibility condition $\mathbf{G}^\top \boldsymbol{\lambda}^0 = \mathbf{e}$. In a post processing we finally recover

$$\boldsymbol{\gamma} = (\mathbf{G}^\top \mathbf{G})^{-1} \mathbf{G}^\top (\mathbf{F}\boldsymbol{\lambda} - \mathbf{d}).$$

and subsequently the desired solution (10).

Following [2] we are going to apply either the lumped preconditioner

$$\mathbf{P}\mathbf{M}^{-1} := \sum_{i=1}^p \mathbf{B}_i \mathbf{K}'_i \mathbf{B}_i^\top, \quad (13)$$

or the Dirichlet preconditioner

$$\mathbf{P}\mathbf{M}^{-1} := \sum_{i=1}^p \mathbf{B}_i \begin{pmatrix} 0 & 0 \\ 0 & \mathbf{S}_i \end{pmatrix} \mathbf{B}_i^\top, \quad (14)$$

where

$$\mathbf{S}_i = \mathbf{K}'_{CC}(u_{i,h}^k) - \mathbf{K}'_{Ci}(u_{i,h}^k) \mathbf{K}'_{ii}^{-1}(u_{i,h}^k) \mathbf{K}'_{iC}(u_{i,h}^k)$$

is the Schur complement of the local finite element matrix \mathbf{K}'_i . Alternatively, one may also use scaled hypersingular boundary integral operator preconditioner as proposed in [8].

4 Numerical Results

In this section we present some examples to show the applicability of this approach for the simulation of biological tissues. First, we consider a strip of an artery layer as shown in Fig. 1 which is decomposed into 40 non-uniform subdomains. To describe the anisotropic and nonlinear material we use the material model (2) with the parameters $\kappa = 20$, $c = 3.0$, $k_1 = 2.36$, $k_2 = 0.84$, $\beta_1 = (0, 0.875, 0.485)^\top$, $\beta_2 = (0, 0.875, -0.485)^\top$. The global nonlinear finite element system with 1.437.285 degrees of freedom is solved by a Newton scheme, where the FETI approach is used in each Newton step. For this specific example the Newton scheme needed 9 iterations. Due to the non-uniformity of the subdomains the efficiency of a global preconditioner becomes more important. Without any preconditioner the global conjugate gradient method exceeded 1.000 iterations to reach a relative error reduction

of 10^{-8} . When using the simple lumped preconditioner (13), about 322 iterations were needed. This calculation lasted about 15 minutes per Newton step on a 32 processor cluster. We observed approximately the same amount of time but less iterations, i.e. 158, when using the Dirichlet preconditioner (14). This is mainly due to the needed calculation of the Schur complements with an involved matrix inversion. Next we consider two examples for more

preconditioner iterations	
none	> 1000
lumped, (13)	322
Dirichlet, (14)	158

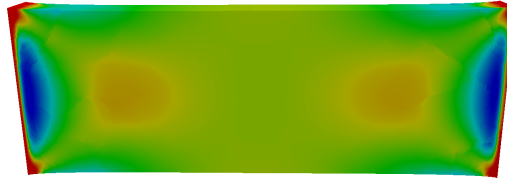


Fig. 1 Van Mises stress of a deformed configuration of an arterial strip.

realistic geometries, see Fig. 2 for a bunny heart with 1.720.854 degrees of freedom which is decomposed into 16 subdomains, and Fig. 3 for a artery bifurcation with 252.942 degrees of freedom and 15 subdomains. In both cases we used the Neo-Hookean material model (3) with $\kappa = 9.17$ and $c = 4.23$.

preconditioner iterations	
none	> 1000
lumped, (13)	265
Dirichlet, (14)	101

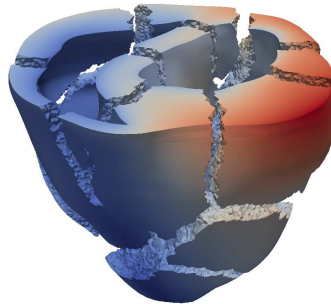


Fig. 2 Displacement field of a bunny heart; numbers of iterations per Newton step.

Acknowledgements This work was supported by the Austrian Science Fund (FWF) and by the TU Graz within the SFB Mathematical Optimization and Applications in Biomedical Sciences. The authors would like to thank G. Holzapfel, G. Of, G. Planck, and C. Pechstein for the fruitful cooperation and many helpful discussions.

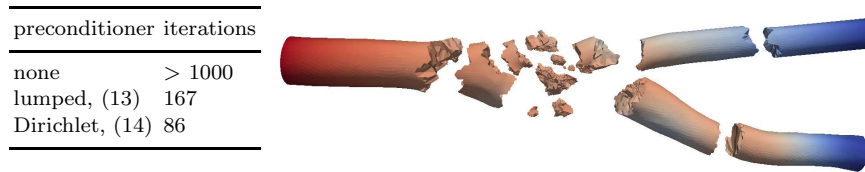


Fig. 3 Displacement field of an artery bifurcation; numbers of iterations per Newton step.

References

- [1] P. G. Ciarlet. *Mathematical elasticity. Vol. I*, volume 20 of *Studies in Mathematics and its Applications*. North-Holland, Amsterdam, 1988.
- [2] C. Farhat, J. Mandel, and F.-X. Roux. Optimal convergence properties of the FETI domain decomposition method. *Comput. Methods Appl. Mech. Engrg.*, 115:365–385, 1994.
- [3] C. Farhat and F.-X. Roux. A method of finite element tearing and interconnecting and its parallel solution algorithm. *Internat. J. Numer. Methods Engrg.*, 32:1205–1227, 1991.
- [4] G. A. Holzapfel. Structural and numerical models for the (visco)elastic response of arterial walls with residual stresses. In G. A. Holzapfel and R. W. Ogden, editors, *Biomechanics of Soft Tissue in Cardiovascular Systems*. Springer, Wien, New York, 2003.
- [5] G. A. Holzapfel, T. C. Gasser, and R. W. Ogden. A new constitutive framework for arterial wall mechanics and a comparative study of material models. *J. Elasticity*, 61:1–48, 2000.
- [6] G. A. Holzapfel and R. W. Ogden. Constitutive modelling of passive myocardium: a structurally based framework for material characterization. *Phil. Trans. Math. Phys. Eng. Sci.*, 367:3445–3475, 2009.
- [7] A. Klawonn and O. Rheinbach. Highly scalable parallel domain decomposition methods with an application to biomechanics. *ZAMM Z. Angew. Math. Mech.*, 90:5–32, 2010.
- [8] U. Langer and O. Steinbach. Boundary element tearing and interconnecting methods. *Computing*, 71:205–228, 2003.
- [9] G. Of and O. Steinbach. The all-floating boundary element tearing and interconnecting method. *J. Numer. Math.*, 7:277–298, 2009.
- [10] A. Toselli and O. B. Widlund. *Domain Decomposition Methods – Algorithms and Theory*. Springer, Berlin, Heidelberg, 2005.